Reprinted from TEXTILE RESEARCH JOURNAL, Vol. 47, No. 10, October 1977
Printed in U. S. A.

Ballistics of Transversely Impacted Fibers

DAVID ROYLANCE

Department of Materials Science and Engineering, Massachusetts Institute of Technology, Cambridge, Massachusetts 02139, U. S. A.

ABSTRACT

The rate-independent theory of transverse impact of textile fibers is reviewed and cast in a form that provides convenient preliminary guidance to designers of impact-resistant textile structures. It is shown that energy-absorption rate increases monotonically with fiber modulus, but that decreased ductility at high modulus may result in an optimum fiber stiffness for transverse critical velocity. A reaction-rate fraction model is suggested as a means of rationalizing the observed variation in experimental transverse critical velocities.

Introduction

Although impact of single fibers or fiber assemblies is an important subject in its own right, being relevant to climbing ropes, aircraft carrier arrest cables, high-speed weaving, etc., the principal developments in this area have been made by workers whose major interests have been in the impact resistance of woven or non-woven textile structures. The most notable of these structures have been the lightweight armor vests used by police and military personnel, but among other important applications can be listed aircraft engine containment shrouds, flak blankets, and vehicle seat belts. Ballistic nylon has been used successfully for these vests since the second world war, although current developments have emphasized the Du Pont aramid fiber marketed as Kevlar[1]. Although, as will be shown below, excellent single-fiber ballistic response does not necessarily guarantee a superior vest, any understanding of textile structure ballistics must be preceeded by an understanding of single-fiber response.

A strong motive for discussing fibers is that single-fiber tests are often used as screening tests for ballistic protection materials. As an example, one often encounters tabulations of "transverse critical velocity," that ballistic velocity at which a transversely impacted yarn experiences nearly instantaneous failure. Typical data is shown below [1].

Transverse critical velocities of textile fibers.

	V_{cr}, m/sec
Nylon	616
Polyester	472
Nomex	442
Fiberglass	274
Kevlar 29	570

[1] Trademark of E. I. du Pont de Nemours & Co., Inc.

Such tests are often indicative of relative ballistic resistance, but perfect correlations cannot be guaranteed; in the above tabulation Kevlar 29 proves to be the best ballistic material when woven into a panel, in spite of its having a lower transverse critical velocity than nylon.

Longitudinal Wave Propagation

Wave propagation phenomena in fibers and thin rods are considerably less complicated than in a general medium, since the possibility of unrestrained transverse contraction in fibers eliminates (to a good approximation) the simultaneous propagation of independent dilatational and distortional waves which are present in general. The equation of motion for fibers or rods is simply [4]:

$$\frac{\partial^2 u}{\partial t^2} = \frac{E}{\rho}\frac{\partial^2 u}{\partial x^2} \quad , \tag{1}$$

where u is the longitudinal particle displacement, ρ is the material density, E is the longitudinal Young's modulus, and x and t are the space and time coordinates. This is the well-known wave equation, whose solution represents a disturbance traveling at a velocity

$$c = \sqrt{E/\rho} \quad . \tag{2}$$

Conventional textile units employing stiffness per unit linear density are very convenient in wave propagation analyses, since the factor ρ is included implicitly in the modulus. For modulus expressed in grams per denier and wavespeed in meters per second, Equation 3 becomes:

$$c = \sqrt{kE} \tag{3}$$

where $k = 88\,260$ is the necessary units-conversion factor. In these equations, as well as those to follow,

the modulus is taken to be the "dynamic" stiffness relevant to the high strain rates corresponding to wave propagation tests. The development of such dynamic constitutive relations from experimental fiber-impact data has been described elsewhere [9].

Consider a fiber fixed at one end whose free end is suddenly subjected to a constant outward velocity V in the longitudinal (fiber) direction. After a time t the strain wave will have propagated into the fiber a distance ct, while the free end will have displaced outward an amount Vt. The strain resulting from the impact is then the displacement Vt divided by the affected length ct:

$$\epsilon = \frac{Vt}{ct} = \frac{V}{c} = \frac{V}{\sqrt{kE}} \quad . \tag{4}$$

The corresponding stress is

$$\sigma = E\epsilon = V\sqrt{\frac{E}{k}} \quad . \tag{5}$$

The above relations have assumed a linear elastic material whose stiffness E is independent of the strain. In this case the wavefront will propagate as a sharp discontinuity (a shock wave) at which the strain rises instantaneously from zero to the value given by Equation 4. Many ballistic fibers are nonlinear, however, and the effect of material nonlinearity leads to some complication of the above description. A nonlinear fiber can be characterized as having a strain-dependent modulus $E = E(\epsilon)$, so that Equation 3 becomes:

$$c = c(\epsilon) = \sqrt{kE(\epsilon)} \quad . \tag{6}$$

The shape of the wavefront is now dependent on the shape of the dynamic stress-strain curve. If the curve is concave toward the strain axis, so that the modulus decreases monotonically with strain, each succeeding increment of strain in the propagating wave travels more slowly than the previous increment. The wave is then dispersive and broadens as it travels. If on the other hand portions of the stress-strain curve are concave away from the strain axis, then portions of the strain wave will overtake more slowly propagating increments of lesser strain, and the wave will contain shock components. In general, a wave may contain both dispersive and shock components.

In the region behind the wave, material flows in the direction of the imposed velocity with a "particle velocity" w. This motion is fed by the strain developed in the propagating wave, and the particle velocity is related to the wave speed by:

$$w = \int_0^{\epsilon_0} c(\epsilon)\mathrm{d}\epsilon = \int_0^{\epsilon_0} \sqrt{kE(\epsilon)}\,\mathrm{d}\epsilon \quad , \tag{7}$$

where ϵ_0 is the ultimate value of strain generated by the impact. Since the particle velocity must match the imposed velocity, we have:

$$V = \int_0^{\epsilon_0} \sqrt{kE(\epsilon)}\,\mathrm{d}\epsilon \quad . \tag{8}$$

The strain ϵ_0 developed by longitudinal impact is found by solving Equation 8, perhaps numerically.

Transverse Impact of Fibers

As the transverse impact of single fibers seems intuitively germane to impact of woven textile panels, the technical community interested in lightweight ballistic protection has devoted intensive effort to this problem since World War II. Following the pioneering works of Taylor [8] and von Karman [5] during the war, valuable contributions have been made by Petterson *et al.* [6], Shultz *et al.* [7], Wilde *et al.* [9], among others, but by far the most prolific of these efforts has been that of Jack C. Smith and his colleagues at the National Bureau of Standards. Reference [3] provides a review of most of this work, which contains a wealth of experimental and theoretical contributions ranging over a period of approximately ten years in the fifties and sixties.

The rate-independent theory of transverse fiber impact as developed by Smith can be stated with reference to Figure 1. This illustrates a fiber, originally straight in the horizontal direction, which has been impacted by a projectile traveling vertically upward. Upon impact, longitudinal waves of the type described in the previous section are propagated outward from the point of impact. Behind these waves material flows inward toward the point of impact at a constant velocity w, strain ϵ_0, and tension σ_0. In addition to the longitudinal waves, transverse "kink" waves are also propagated outward from the impact point. At the transverse wavefront the inward material flow ceases abruptly and is replaced by a transverse particle velocity equal in magnitude and direction to that of the projectile. The strain and tension are unchanged across the transverse wavefront, but both the longitudinal and transverse particle velocities experience discontinuities there; in this sense the transverse wave is a geometrical shock. The apparently unbalanced tensions on either side of the transverse wavefront are compensated by the change in particle momentum as the wave propagates. Behind the transverse wavefront all particle velocities are equal in magnitude and direction to the projectile velocity, and the fiber configuration is a straight line at a constant inclination θ from the longitudinal direction.

The inward particle velocity is found, as in the longitudinal case, as

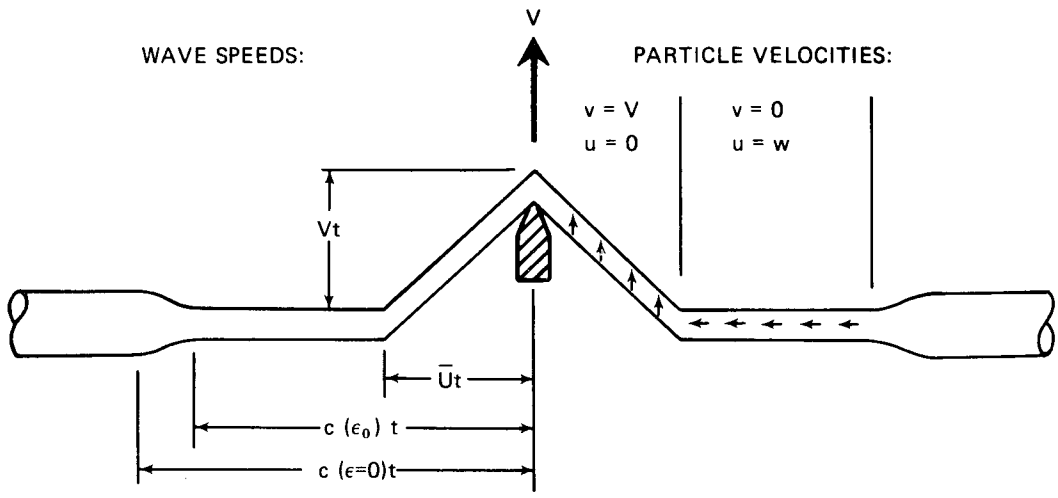

FIG. 1. Wave propagation in a transversely impacted fiber.

$$w = \int_0^{\epsilon_0} c(\epsilon)\mathrm{d}\epsilon = \int_0^{\epsilon_0} \sqrt{kE(\epsilon)}\,\mathrm{d}\epsilon \quad . \tag{9}$$

The final strain ϵ_0 is unknown as yet, but of course $E(\epsilon)$ is known as the slope of the stress-strain curve. The outward velocity U of the transverse kink wave, measured relative to a Lagrangian frame attached to and extending with the fiber, is

$$U = \sqrt{\sigma_0 k/(1 + \epsilon_0)} \quad , \tag{10}$$

where σ_0 is the ultimate value of tension (in g/den for $k = 88{,}260$) induced by the impact. To a fixed observer the transverse wave appears to propagate in a "laboratory" frame of reference at:

$$\bar{U} = (1 + \epsilon_0)U - w \quad . \tag{11}$$

Finally, the above variables are related to the impact velocity V through the relation:

$$V = \sqrt{(1 + \epsilon_0)^2 U^2 - \bar{U}^2} \quad . \tag{12}$$

Equations 9–12 constitute four relations between V, w, ϵ_0, σ_0, U, and $\bar{U}$. The material dynamic stress-strain curve relates σ_0 and ϵ_0, so that once one of the parameters (say V) is specified, the other four independent parameters (w, ϵ_0, U, $\bar{U}$) can be found. For nonlinear stress-strain curves, numerical solutions will likely be more convenient.

Certain limitations to the Smith analysis described above must be mentioned. First, it is rate-independent. Most polymeric fibers exhibit strong rate dependencies, and these effects are beyond the capacity of this analysis to describe. Perhaps a more severe limitation is that the Smith analysis is not applicable to late-time effects in the wave propagation process. In real situations the outgoing longitudinal wave soon collides with an obstacle: a clamp, in the case of single-fiber tests, or a fiber crossover, in the case of impact in woven textile panels. Upon such a collision a reflected wave is propagated from the collision point in the direction opposite that of the original wave. This reflected wave in turn soon collides with the outward-traveling transverse wave, and this collision generates another two waves which travel away from the collision point. These waves in turn eventually collide with the clamps, or the projectile, or other waves. The result of these wave reflections and interactions is a situation which becomes intractable by closed-form mathematical methods, and this late-time intractability is a principal reason for the development of numerical computer solutions.

Use of the Rate-Independent Theory in Preliminary Design

In spite of the limitations of the Smith theory outlined above, the rate-independent analysis provides a highly useful means of assessing approximate relations between fiber material properties and ballistic response. These relations are of considerable value in performing preliminary design steps in development of textile ballistic-protection devices.

Assuming the material to be linear in stress-strain response (E = constant), the Smith analysis can be cast in the simple form:

$$V = \sqrt{\epsilon_0 kE[2\sqrt{\epsilon_0(1 + \epsilon_0)} - \epsilon_0]} \quad , \tag{13}$$

which provides a relation for the strain ϵ_0 developed by impact at a velocity V in terms of the fiber modulus. This relation can be solved numerically if one wishes to compute ϵ_0 for a given V, or it can be used directly to plot ϵ_0 *versus* V for the purpose of developing design curves (see Fig. 2). Once ϵ_0 is known, then σ_0, U, $\bar{U}$, and w can be found from either the stress-strain relation

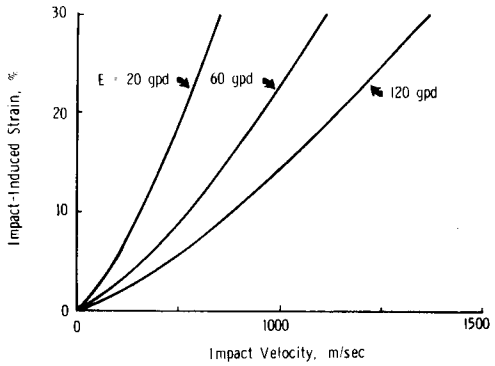

FIG. 2. Predicted impact strain for linear rate-independent fibers.

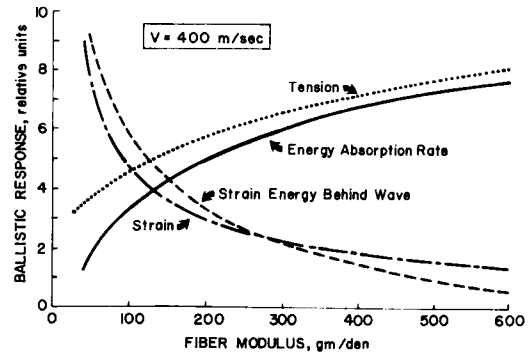

FIG. 4. Effect of fiber stiffness on ballistic response; 10 = 10 g/den for tension, 10% for strain, 0.03 g/den for strain energy, and 900 g m/den sec for energy absorption rate.

or Equations 9–12. Figure 3 shows such a plot of tension σ_0 *versus* V with modulus as a parameter.

Since the above curves rise monotonically with velocity, one can observe the influence of modulus more easily by plotting ballistic response at a constant velocity, and Figure 4 shows such a plot at $V = 400$ m/sec. Here are plotted the strain and tension from the above methods, along with the strain energy $\gamma = \frac{1}{2}\sigma_0\epsilon_0$ developed behind the wave and the rate of energy absorption γc of the fiber. (The term γc is shown in mixed units, but it could be converted to joules/sec once the density and denier of the fiber are specified.) The rate of energy absorption at the wavefront must equal the rate at which the fiber extracts kinetic energy from the projectile, and it is a reasonable measure of ballistic efficiency. Note that this energy-absorption rate rises monotonically with fiber modulus, although with less dramatic improvements after approximately 500 g/den.

Of course, one cannot improve ballistic efficiency indefinitely by continuing to seek stiffer fibers. In general, increases in stiffness are accompanied by decreases in breaking strain, and a point may well be reached where this reduced ductility overshadows the beneficial reduction in impact-genreated strain shown in Figure 2. This effect may be quantified by means of Equation 13, where one may calculate the critical transverse velocity by determining the velocity which just generates the dynamic breaking strain on impact. If one knows the variation of breaking strain with stiffness, these calculations may be used to select approximately an optimum fiber stiffness for ballistic efficiency. This process is carried through for illustrative purposes in Figure 5.

The dashed line in this figure is the relation between dynamic stiffness and breaking strains as determined from fiber-impact tests on a series of nylon yarns that

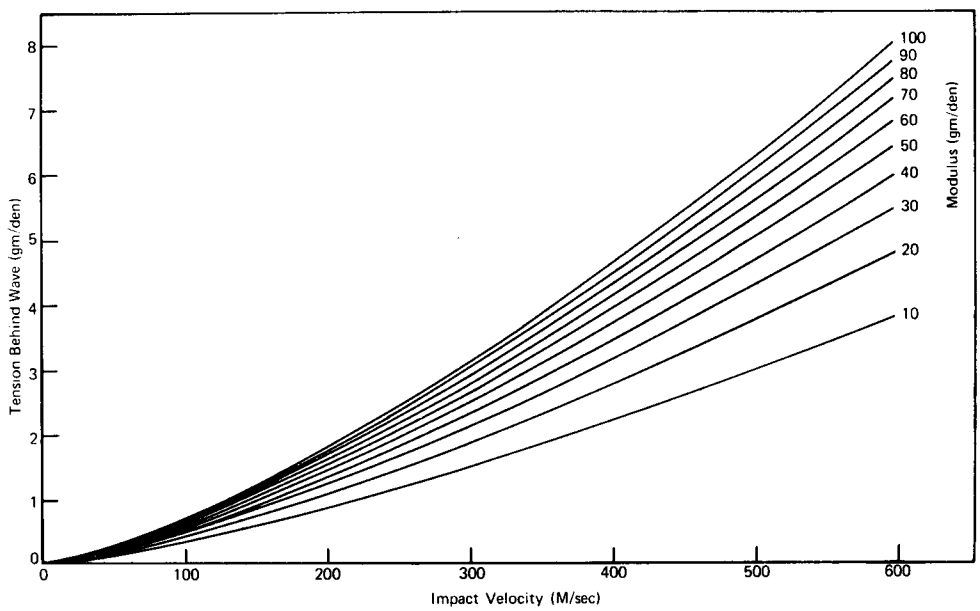

FIG. 3. Predicted impact tension for linear rate-independent fibers.

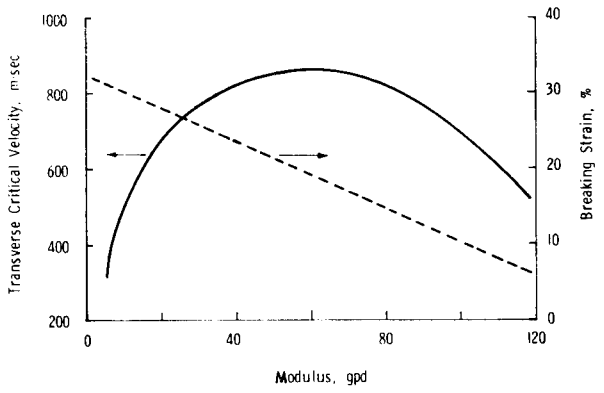

FIG. 5. Prediction of optimum stiffness for nylon fibers.

had been subjected to various drawing treatments by the manufacturer [9]. The solid line is then the calculated transverse critical velocity, considering the effect of stiffness on both impact-induced strain and on breaking strain. An optimum is observed near 60 g/den, which is in fair agreement with experimental observation. All this is a quantification of the often-quoted guideline in armor design that one seeks the highest possible modulus in order to spread the impact over a wide area *via* increased wavespeed, but that the process must not be carried so far as to induce excessive brittleness. In hard armor this reasoning has led to the use of ceramic faceplates to give high wavespeed, backed by a fiberglass laminate to provide the needed toughness.

Selection of a Failure Criterion

The use of a simple ultimate breaking strain as a failure criterion in the above example is overly simplistic, since it does not incorporate the strong temperature and rate dependencies that are known to exist in polymeric materials. A commonly encountered fracture model which does incorporate these dependencies and is still computationally convenient is that due to Zhurkov [10], which states that the lifetime τ of a solid subjected to a uniaxial stress σ is of the form

$$\tau = \tau_0 \exp\left[\frac{U^* - \gamma^*\sigma}{RT}\right] , \qquad (14)$$

where τ_0 is a pre-exponential factor with units of time, U^* is an apparent activation energy for the fracture process, γ^* is a factor with units of volume, R is the gas constant (1.987×10^{-3} kcal/mole °K), and T is the absolute temperature. For constant temperature, Equation 14 reduces to

$$\tau = \alpha \exp(-\beta\sigma) , \qquad (15)$$

where

$$\alpha = \tau_0 \exp(U^*/RT) ,$$
$$\beta = \gamma^*/RT . \qquad (16)$$

When stress and temperature vary during the loading process, one can assume linear superposition and write the Zhurkov criterion in the form:

$$\int_0^\tau \frac{dt}{\tau_0 \exp\left[\dfrac{U^* - \gamma^*\sigma(t)}{RT(t)}\right]} = 1 . \qquad (17)$$

In a constant-stress-rate experiment at constant temperature, for instance,

$$\sigma(t) = Ct$$

$$\int_0^\tau \frac{dt}{\alpha \exp(-\beta C t)} = 1$$

$$\frac{\exp(\beta C\tau) - 1}{\alpha\beta C} = 1$$

$$\tau = \frac{\ln(1 + \alpha\beta C)}{\beta C} . \qquad (18)$$

To illustrate the order of rate dependency provided by Zhurkov's model, Figure 6 shows a plot of Equation 18 for the case of drawn nylon fibers. In this figure $\alpha = 2.20 \times 10^{19}$ sec, and $\beta = 5.13$ (g/den)$^{-1}$; these are the values obtained by Zhurkov [10] by fitting Equation 15 to creep-rupture data. Such a plot can be used to depict the time-to-break for a fiber, and the tenacity-at-break, as a function of the loading rate.

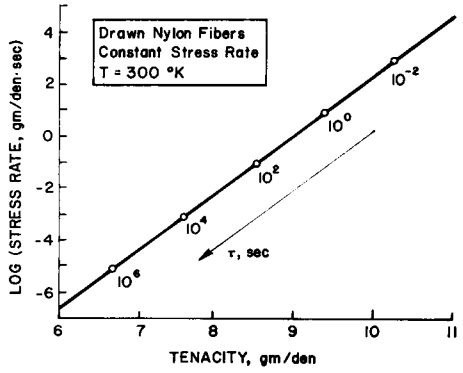

FIG. 6. Variation of breaking tenacity with loading rate—Zhurkov model.

As a more direct example of the utilization of Zhurkov's model in fiber ballistics, the stress predicted by the Smith theory for a given impact velocity and fiber modulus can be used in Equation 14 to predict the time after impact at which the fiber will rupture. This analysis predicts that there is no unique critical transverse velocity, but rather a range of velocities over which the fiber will fail in experimentally observa-

ble times. Figure 7 shows the predicted results for drawn nylon fibers, using an assumed dynamic modulus of 80 g/den with the same values of α and β used in Figure 6. This figure shows that at velocities above approximately 775 m/sec, rupture occurs in less than fifty microseconds and would be counted in most high-speed photographic records as having occurred instantaneously upon impact. The times-to-break become exponentially longer at lower velocities, and failure will occur at the clamp due to wave reflection at times dependent on the wavespeed and fiber length. It is the variation in what may be termed a critical velocity for impact which may make up a large part of the scatter observed experimentally in determining critical transverse velocities.

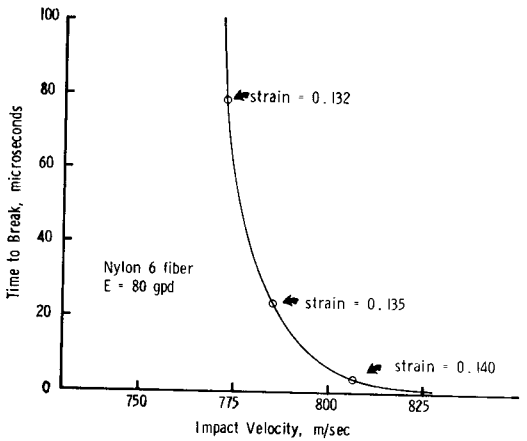

FIG. 7. Variation in transverse critical velocity due to fracture rate effects.

An important advantage to Zhurkov's model is that it is derivable in terms of basic reaction-rate fracture analysis. As such, it provides a means whereby the materials scientist can predict materials and processing modifications so as to manipulate the fracture parameters and improve ballistic performance. A recent review [2] describes the basic implications of reaction-rate models such as Zhurkov's, as well as their limitations and experimental corroboration. Suffice it to say that the development of these models is somewhat controversial, with several quite divergent approaches having strong advocates. Zhurkov's model in particular is often criticized as being simplistic, but is convenient for use in impact analysis by virtue of its computational convenience and its ability to model a wide range of materials behavior, if only phenomenologically. Finally, it should be cautioned that the experiments Zhurkov used in corroborating his model were no faster than the millisecond time scale, some three orders of magnitude slower than ballistic impact fractures. Such an extrapolation is clearly dangerous and should be verified by additional experimentation. The plot given in Figure 7 is in reasonable but not excellent agreement with experimental data given in Smith's papers, indicating that the approach is promising but needing of further corroboration.

Acknowledgments. This work was supported by the U. S. Army Natick Research and Development Command under Contract DAAG17-76-C-0013, and the U. S. Army Research Office under Contract DAAG29-76-C-0044.

Literature Cited

1. Coskren, R. J., Abbott, N. J., and Ross, J. H., "Kevlar 29 and 49 in Parachute Fabrics," AIAA Paper No. 75-1360, November, 1975.
2. DeVries, K. L. and Roylance, D. K., The Observation of Molecular Bond Rupture During Fracture in Polymers, *Progress in Solid State Chemistry* **8**, 283 (1973).
3. Fenstermaker, C. A. and Smith, J. C., Stress-Strain Properties of Textile Yarns Subjected to Rifle Bullet Impact," *Appl. Poly. Symp. No. 1*, 125 (1965).
4. Kolsky, H., "Stress Waves in Solids," Dover Publications, New York, 1963.
5. von Karman, T. and Duwez, P., The Propagation of Plastic Deformation in Solids, *J. Appl. Phys.* **21**, 987 (1950).
6. Petterson, D. R., Stewart, G. M., Odell, F. A., and Maheux, R. C., Dynamic Distribution of Strain in Textile Materials Under High-Speed Impact, *Textile Res. J.* **30**, 411 (1960).
7. Shultz, A. B., Tuschak, P. A., and Vicario, A. A., Experimental Evaluation of Material Behavior in a Wire Under Transverse Impact, *J. Appl. Mech.*, 392 (June, 1967).
8. Taylor, G. I., "*Scientific Papers of G. I. Taylor*," Vol. 1, Paper No. 32, Cambridge University Press, England, 1958.
9. Wilde, A. F., Ricca, J. J., Roylance, D. K., Tocci, G. C., and Rogers, J. M., "Deformation and Rupture of Fibers and Films Under Missile Impact," Technical Report AMMRC 72-12, Army Materials and Mechanics Research Center, Watertown, Massachusetts, May 1972.
10. Zhurkov, S. N., Kinetic Concept of the Strength of Solids *Intl. J. Fracture Mech.* **1**, 311 (1965).

Manuscript received February 4, 1977.